Available online at www.sciencedirect.com
SCIENCE DIRECT®

Journal of Nuclear Materials 346 (2005) 220–225

journal of nuclear materials

www.elsevier.com/locate/jnucmat

A new model of grain growth kinetics in UO_2 fuel pellets. Part 2: Normal grain growth kinetics controlled by pore migration

M.S. Veshchunov *

Nuclear Safety Institute, Russian Academy of Sciences, 52, B. Tulskaya, Moscow 115191, Russia

Received 1 February 2005; accepted 10 June 2005

Abstract

The grain growth model presented in Part 1 is further developed and applied to the analysis of the normal grain growth kinetics controlled by pore migration during fresh UO_2 thermal treatment (sintering). Additional consideration of fuel densification (i.e. porosity reduction) allows explanation of complicated grain growth kinetics characterised by non-integer growth exponents observed in recent tests.

1. Introduction

The model of the grain growth presented in Part 1 can be extended to modelling the normal grain growth kinetics of non-irradiated porous UO_2 fuel, experimentally studied in the annealing tests, e.g. [1–3].

In the pure systems without porosity under isothermal conditions the grain growth can be satisfactorily described by parabolic kinetics:

$$\overline{R}^2_{\mathrm{gr}}(t) - \overline{R}^2_{\mathrm{gr}}(0) = K(T)t, \tag{1}$$

where $\overline{R}_{\mathrm{gr}}(0)$ and $\overline{R}_{\mathrm{gr}}(t)$ are the average grain radii of the sample before annealing and after an annealing time t at a temperature T, respectively. This relationship can be derived by direct integration of Eq. (7) in Part 1:

$$\bar{v}^{(0)}_{\mathrm{gb}} = \frac{\mathrm{d}\overline{R}_{\mathrm{gr}}}{\mathrm{d}t} = M\frac{1}{\overline{R}_{\mathrm{gr}}}. \tag{2}$$

Grain growth in the final stage of UO_2 fuel sintering is the result of interactions between grain boundaries and residual porosity. Pores on the grain boundaries give rise to drag effect which impedes boundary motion. In the majority of experimental studies [2,3] grain growth was approximated by a more slow kinetic equation:

$$\overline{R}^n_{\mathrm{gr}}(t) - \overline{R}^n_{\mathrm{gr}}(0) = K't \tag{3}$$

with the growth exponent $n = 3$ or 4. Recently it was revealed that in many cases the grain growth kinetics must be described by non-integer exponents, somewhat different from 3 or 4 [1].

2. Phenomenological consideration

For explanation of the measured kinetics described by Eq. (2) with integer exponents, a series of models

---

* Tel.: +7 095 955 2218; fax: +7 095 958 0040.
E-mail address: vms@ibrae.ac.ru

0022-3115/$ - see front matter © 2005 Elsevier B.V. All rights reserved.
doi:10.1016/j.jnucmat.2005.06.010

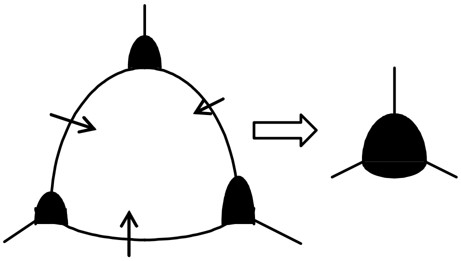

Fig. 1. Pore migration with boundaries and resulting pore growth during normal grain growth (from [4]).

has been proposed, most of them based on consideration of Kingery and Francois [4]. They assumed that, as grains are removed in the growth process, pores migrating with the boundaries are brought together, and pore growth occurs together with grain growth, see Fig. 1. After, say, twofold increase of the mean grain size, an amount of grains N_{gr} decreases by one order of magnitude ($N_{gr} \propto \overline{R}_{gr}^{-3}$), and practically all pores are located at grain corners, so amount of pores N_p becomes proportional to the amount of grains, $N_p \propto N_{gr}$.

Kingery and Francois additionally assumed that in the later stages of sintering grain growth is relatively faster than fuel densification, so that the pore fraction remains essentially constant. Under such an assumption, the mean pore radius $\overline{R}_p \propto N_p^{-1/3}$ and thus is proportional to the mean grain radius:

$$\overline{R}_p \propto \overline{R}_{gr}. \tag{4}$$

On this basis, to account for drag effect of the pores, they proposed to introduce an additional factor $\overline{R}_p^{-1} \propto \overline{R}_{gr}^{-1}$ in the r.h.s of Eq. (2), leading to Eq. (3) with $n = 3$ after integration.

Later Nichols [5] derived a more appropriate equation for the drag force, Eq. (13) in Part 1, which was applied by Brook [6,7] to consideration of normal grain growth kinetics controlled by pore migration. Using this equation for the later stages of sintering when corner pore mobility controls boundary movement, Brook obtained an equation:

$$\frac{d\overline{R}_{gr}}{dt} \propto \frac{B_p}{\overline{R}_{gr} n_p}, \tag{5}$$

where n_p is the surface concentration of pores on the boundary, and pore mobility:

$$B_p \propto \overline{R}_p^{-n}, \tag{6}$$

is determined by migration mechanism, i.e. $n = 3$ for the mechanisms of lattice diffusion and gas phase transport at $P = \text{const.}$, and $n = 4$ for the surface diffusion mechanism. He also noticed that for the considered situation where pores are located at grain corners, their separation is proportional to $\overline{R}_{gr}$, so the surface concentration of pores on the boundary is inversely proportional to $\overline{R}_{gr}^{-2}$:

$$n_p \propto \overline{R}_{gr}^{-2}. \tag{7}$$

Substitution of Eqs. (6) and (7) in Eq. (5) results in:

$$\frac{d\overline{R}_{gr}}{dt} \propto \overline{R}_{gr}^{1-n}, \tag{8}$$

or, after its integration:

$$\overline{R}_{gr}^n(t) - \overline{R}_{gr}^n(0) = K't. \tag{9}$$

Therefore, namely the pore migration mechanisms by lattice diffusion and gas phase transport at $P = \text{const.}$ provide grain growth kinetics with $n = 3$, whereas $n = 4$ is afforded by the surface diffusion mechanism.

Nevertheless, Bourgeois et al. [1] recently noticed that to describe grain growth in their recent tests, the slope $\ln(\overline{R}_{gr}^n(t) - \overline{R}_{gr}^n(0))$ as a function of $\ln t$ might be quite different from 1, whether with $n = 3$ or $n = 4$, and also from one temperature to another. Therefore, in order to describe grain growth in these cases, a non-integer exponent n must be used.

In order to explain such a behaviour, one should take into account that Eq. (9) was derived under simplifying assumption that the pore fraction remains essentially constant during grain growth, $N_p\overline{R}_p^3 = \text{const.}$ However, this assumption was not confirmed in the new tests [1]. Indeed, in these tests changes in density of fuel pellets during heat treatment were monitored simultaneously with the grain growth measurements, which demonstrated a plain correlation between grain growth and fuel densification, Figs. 2(a) and 3(a).

It is straightforward to recalculate this correlation in terms of porosity reduction versus grain size growth at various test temperatures, as presented in Figs. 2(b)–(d) and 3(b)–(d) for batches with different porosities, T0 and T12, respectively. Analysis of experimental points shows that relative porosity of fuel pellets, $V_{pores}/V_0 = N_p(t)\overline{R}_p^3(t)/N_p(0)\overline{R}_p^3(0)$, can be fairly correlated with the mean grain size, $\overline{R}_{gr}(t)/\overline{R}_{gr}(0)$, by a power dependence:

$$V_{pores}/V_0 = (\overline{R}_{gr}(t)/\overline{R}_{gr}(0))^{-a} \tag{10}$$

with parameter $a \approx 0.2$–0.3 slightly dependent on temperature and somewhat different for two batches T0 and T12, as seen from Figs. 2 and 3.

Under the main assumption $N_p \propto N_{gr} \propto \overline{R}_{gr}^{-3}$ one can see from Eq. (10):

$$V_{pores}/V_0 \propto N_p\overline{R}_p^3 \propto \overline{R}_p^3/\overline{R}_{gr}^3 \propto \overline{R}_{gr}^{-a}. \tag{11}$$

In this case the above presented relationship between mean radii of pores and grains, Eq. (4), is violated and takes the form:

$$\overline{R}_p(t)/\overline{R}_p(0) = (\overline{R}_{gr}(t)/\overline{R}_{gr}(0))^{1-a/3}. \tag{12}$$

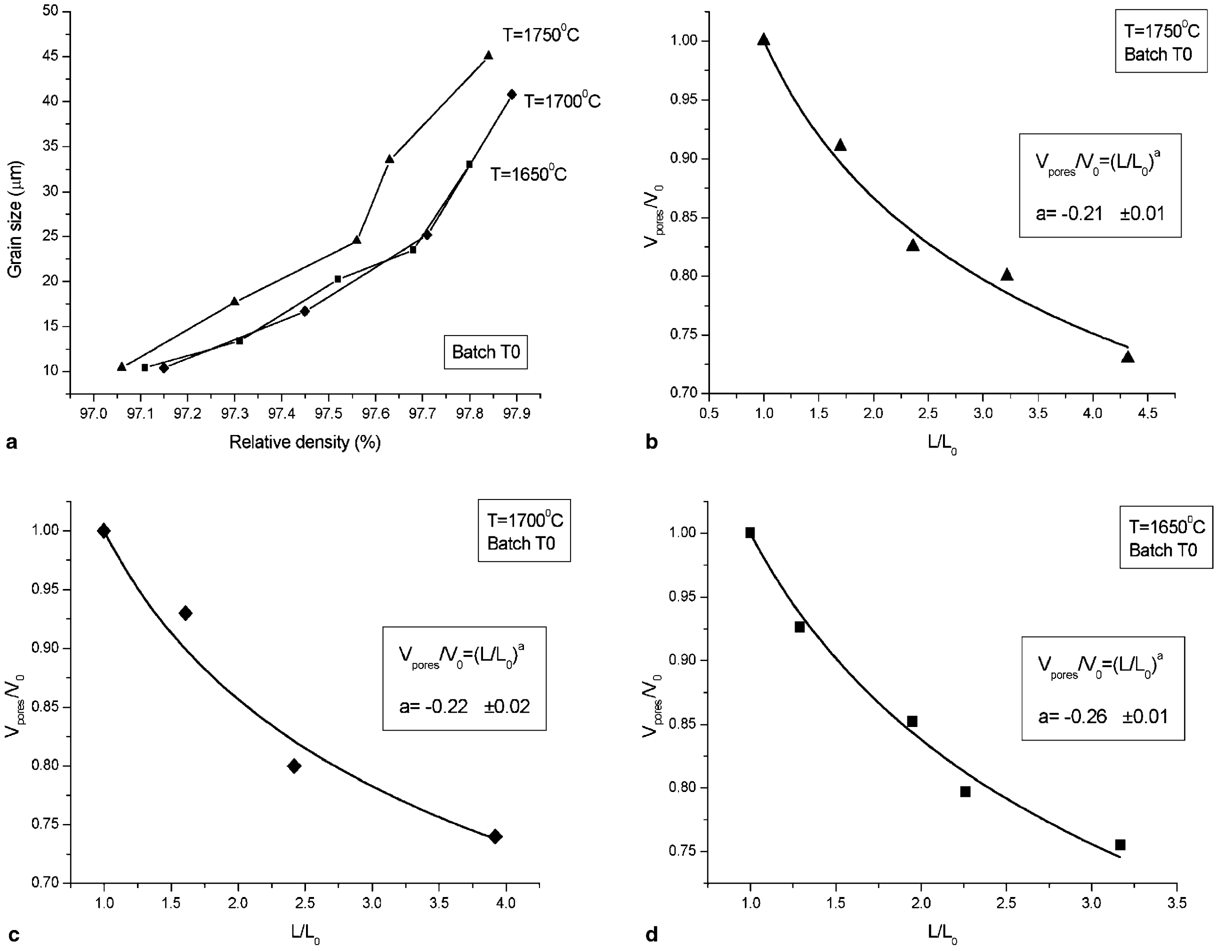

Fig. 2. (a) Variation of grain size as a function of relative density during annealing of batch T0, measured in [1]. (b) Variation of fuel porosity V_{pores} as a function of grain size L, recalculated from (a) and fitted by analytical curve, for batch T0 at 2023 K. (c) Variation of fuel porosity V_{pores} as a function of grain size L, recalculated from (a) and fitted by analytical curve, for batch T0 at 1973 K. (d) Variation of fuel porosity V_{pores} as a function of grain size L, recalculated from (a) and fitted by analytical curve, for batch T0 at 1923 K.

Substituting Eqs. (12) and (7) in Eq. (5) one can get, instead of Eq. (8):

$$\frac{\mathrm{d}\overline{R}_{\mathrm{gr}}}{\mathrm{d}t} \propto \overline{R}_{\mathrm{gr}}^{1-n(1-a/3)}, \tag{13}$$

or, after integration of Eq. (13):

$$\overline{R}_{\mathrm{gr}}^{n(1-a/3)}(t) - \overline{R}_{\mathrm{gr}}^{n(1-a/3)}(0) = K(T)t. \tag{14}$$

This means that for the surface diffusion mechanism of pores (i.e. $n = 4$) the power exponent attains non-integer value ≈3.6–3.7, whereas for lattice and/or gas phase diffusion (i.e. $n = 3$) it becomes ≈2.7–2.8.

In order to calculate the new exponent a from the theory, one should consider self-consistently two processes of corner pores coalescence due to grain growth and pore size reduction due to vacancies evaporation in the course of thermal annealing (or irradiation induced densification). Consideration of this problem is presented in Section 3.

3. Microscopic consideration

The grain growth model is considerably simplified by an assumption of spherical grains. However, an accurate treatment of extra-granular porosity requires more adequate grain shape specification. In a more realistic approach the shape of UO_2 grains is considered as truncated octahedron or tetrakaidecahedron (TDK) [8]. The TDK has 14 faces, six of which are square and eight hexagonal, 36 edges and 24 corners. When packed together an array of TDKs can fill all available space in a solid

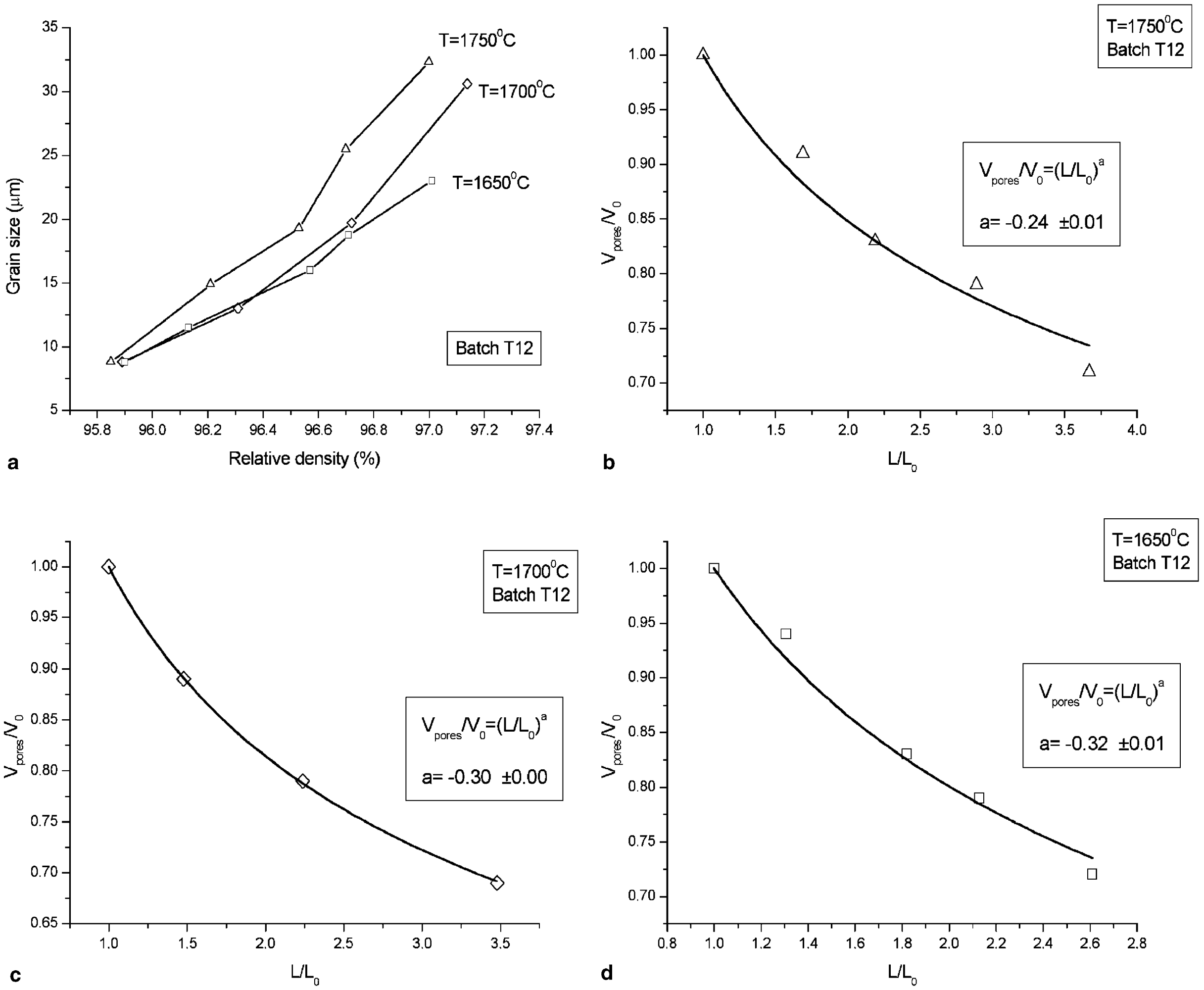

Fig. 3. (a) Variation of grain size as a function of relative density during annealing of batch T12, measured in [1]. (b) Variation of fuel porosity V_{pores} as a function of grain size L, recalculated from (a) and fitted by analytical curve, for batch T12 at 2023 K. (c) Variation of fuel porosity V_{pores} as a function of grain size L, recalculated from (a) and fitted by analytical curve, for batch T12 at 1973 K. (d) Variation of fuel porosity V_{pores} as a function of grain size L, recalculated from (a) and fitted by analytical curve, for batch T12 at 1923 K.

and thus represents an appropriate basic building block. The meeting point of each grain face is shared by two grains, each grain edge by three grains and each grain corner by four grains. Grain corner bubbles are constructed by intersection of four spherical surfaces and in shape are close to the spherical ones. For the simplicity, in the MFPR code these corner bubbles are assumed to have a spherical form.

Shrinkage of an isolated pore owing to vacancies evaporation during thermal annealing can be calculated by application of the Speight and Beere's approach [9] (for the grain face cavities) to the case of the corner pore, which is located at intersection of 6 grain faces (4 hexagonal and 2 square):

$$\frac{\partial V_{\mathrm{p}}}{\partial t} \approx -\frac{3.67\pi\Omega D_{\mathrm{gb}} w}{\beta kT}\,\frac{2\gamma_{\mathrm{s}}}{R_{\mathrm{p}}}, \qquad (15)$$

where D_{gb} is the grain boundary self-diffusion coefficient of uranium atoms, $\beta = \ln(R_{\mathrm{c}}/R_{\mathrm{p}}) - 0.25(1 - R_{\mathrm{c}}^2/R_{\mathrm{p}}^2) \times (3 - R_{\mathrm{c}}^2/R_{\mathrm{p}}^2)$ is the dimensionless factor, $2w$ is the effective thickness of the grain boundary ($\sim$1 nm), $(\pi R_{\mathrm{c}}^2)^{-1} = n_{\mathrm{p}}$ determines the radius of the pore sinking zone R_{c}, which can be estimated taking into account that 24 corners are distributed over the grain surface with the area of $\approx 4\pi R_{\mathrm{gr}}^2$, i.e.

$$n_{\mathrm{p}} \approx 6/\pi R_{\mathrm{gr}}^2 \quad \text{and} \quad R_{\mathrm{c}} \approx R_{\mathrm{gr}}\Big/\sqrt{6}, \qquad (16)$$

where n_p is the surface concentration of corner pores on the boundary.

Therefore, decrease of an isolated pore radius can be evaluated as

$$\frac{\partial R_p}{\partial t} \approx -\frac{5.5\Omega D_{gb} w}{\beta kT}\frac{\gamma_s}{R_p} \equiv -\frac{\alpha}{R_p}, \tag{17}$$

where

$$\alpha = \frac{5.5\Omega D_{gb} w\gamma_s}{\beta kT}. \tag{18}$$

Neglecting pores shrinkage, one can obtain (following Kingery and Francois [4]) that variation of total porosity in the course of pores coalescence is zero, $\frac{d(N_p\overline{V}_p)}{dt} = 0$. However, taking pores shrinkage into consideration, Eq. (15), one will obtain that in this case

$$\frac{d(N_p\overline{V}_p)}{dt} = N_p\frac{\partial \overline{V}_p}{\partial t}, \tag{19}$$

where

$$\frac{d(N_p\overline{V}_p)}{dt} = N_p\frac{d\overline{V}_p}{dt} + \overline{V}_p\frac{dN_p}{dt} \tag{20}$$

and

$$N_p \propto N_{gr} \propto \overline{R}_{gr}^{-3}. \tag{21}$$

Here $\frac{\partial \overline{V}_p}{\partial t}$ denotes variation of the pore mean volume owing solely to pores shrinkage, Eq. (15), whereas $\frac{d\overline{V}_p}{dt}$ denotes total variation of the pore mean volume owing to pores simultaneous shrinkage and coalescence.

Substituting Eqs. (15), (20) and (21) in Eq. (19), one obtains

$$\frac{d\overline{R}_p}{dt} - \frac{\overline{R}_p}{\overline{R}_{gr}}\frac{d\overline{R}_{gr}}{dt} = -\frac{\alpha}{3\overline{R}_p^3}. \tag{22}$$

In the case when the corner pore mobility controls grain boundary movement, the relationship for the mean grain radius growth controlled by pore mobility, Eq. (14) in Part 1, takes the form:

$$\frac{d\overline{R}_{gr}}{dt} \approx \frac{8}{81}\frac{\gamma_{gb}\xi}{\overline{R}_{gr}}\frac{B_p}{n_p} \approx 0.1\frac{\gamma_{gb}\xi}{\overline{R}_{gr}}\frac{B_p\pi\overline{R}_{gr}^2}{6}, \tag{23}$$

where Eq. (16) was used for n_p.

As shown in Part 1, for the considered case of large pores with $R_p \geqslant 1\ \mu m$ the surface diffusion mechanism controls the pore migration kinetics, therefore, in accordance with Eq. (52) in Part 1, $B_p \approx \frac{3D_s w\Omega}{2\pi kTR_p^4}$. Substituting this value in Eq. (23), finally one obtains:

$$\frac{d\overline{R}_{gr}}{dt} \approx \frac{\gamma_{gb}\xi}{40}\frac{D_s w\Omega}{kT}\frac{\overline{R}_{gr}}{\overline{R}_p^4}, \tag{24}$$

or

$$\frac{d\overline{R}_{gr}}{dt} = \varphi\frac{\overline{R}_{gr}}{\overline{R}_p^4}, \tag{25}$$

where

$$\varphi \approx \frac{\gamma_{gb}\xi}{40}\frac{D_s w\Omega}{kT}. \tag{26}$$

The system of Eqs. (22) and (24):

$$\frac{d\overline{R}_p}{dt} - \frac{\overline{R}_p}{\overline{R}_{gr}}\frac{d\overline{R}_{gr}}{dt} = -\frac{\alpha}{3\overline{R}_p^3},$$

$$\frac{d\overline{R}_{gr}}{dt} = \varphi\frac{\overline{R}_{gr}}{\overline{R}_p^4},$$

has the solution:

$$\overline{R}_p \propto \overline{R}_{gr}^{(1-\alpha/3\varphi)} \tag{27}$$

and

$$\overline{R}_{gr}^{4(1-\alpha/3\varphi)}(t) - \overline{R}_{gr}^{4(1-\alpha/3\varphi)}(0) = Kt. \tag{28}$$

The total porosity reduction can be calculated as $V_{pores} = N_p\overline{V}_p \propto N_p\overline{R}_p^3 \propto \left(\frac{\overline{R}_p}{\overline{R}_{gr}}\right)^3$ and after substitution of Eq. (27):

$$V_{pores} = N_p\overline{V}_p \propto \overline{R}_{gr}^{-\alpha/\varphi} = \overline{R}_{gr}^{-a}, \tag{29}$$

where $a = \alpha/\varphi$.

Substituting Eqs. (18) and (26) in Eq. (29), one can evaluate:

$$a = \alpha/\varphi \approx \frac{220}{\xi\beta}\frac{D_{gb}}{D_s}, \tag{30}$$

where $\xi \approx 1$–2, parameter β depends on the fuel porosity (see designations after Eq. (15)) and for the fuel density 96–98% varies in the range 0.2–0.3.

4. Comparison with the experiment

Owing to a large uncertainty in determination of the diffusion coefficients (especially D_s [1]), it is difficult to evaluate the exponent a directly from Eq. (30). In this situation it seems more reasonable to demonstrate that dependencies of this exponent on temperature and sample porosity follow correct trend with respect to test observations.

First of all, substituting the evaluated exponent $a \approx 0.2$–0.3 (see Figs. 2 and 3) in Eq. (30), one can estimate the ratio $D_s/D_{gb} \approx (2–5) \times 10^3$, in a reasonable agreement with experimental data, see Section 3.3 in Part 1.

Applying Eq. (30) to two batches T0 and T12 with different mean (during the test) densities ≈96.5% ($\beta \approx 0.25$) and ≈97.5% ($\beta \approx 0.32$), respectively, one obtains $a(\mathrm{T0})/a(\mathrm{T12}) \approx 0.78$, in a reasonable agreement with measurements at all three test temperatures: at 1923 K, $a(\mathrm{T0})/a(\mathrm{T12}) \approx 0.81$, at 1973 K,

$a(\mathrm{T0})/a(\mathrm{T12}) \approx 0.73$ and at 2023 K, $a(\mathrm{T0})/a(\mathrm{T12}) \approx 0.87$, as can be seen from Figs. 2 and 3.

Eq. (30) also qualitatively correctly predicts the temperature dependence of the exponent a. Indeed, using experimentally measured activation energies for the diffusion coefficients $D_{\mathrm{gb}} \propto \exp(-35\,250/T)$ [10] and $D_{\mathrm{s}} \propto \exp(-450\,000/RT) = \exp(-54\,125/T)$ [11], one can estimate the ratio $a(1973\ \mathrm{K})/a(2023\ \mathrm{K}) \approx 1.62$. Taking into account the uncertainty of the diffusion coefficients evaluation, this prediction is in a fair agreement with measurements either for batch T0 ($\approx$1.24), or for batch T12 ($\approx$1.33), as can be seen from Figs. 2 and 3.

5. Conclusions

The new model for the grain growth is further developed for consideration of unirradiated porous UO_2 pellets.

Being applied to analysis of the normal grain growth kinetics during fresh UO_2 thermal treatment (sintering) with additional consideration of observed fuel densification (i.e. porosity reduction), the model predicts for the first time that the grain growth kinetics controlled by pore migration can be characterised by non-integer growth exponents, in accordance with recent observations of Bourgeois et al. [1].

The model qualitatively correctly describes the main trends in dependence of the growth exponents on temperature and fuel porosity measured in the tests [1].

Acknowledgments

This work was supported by IRSN, Cadarache (France) under the Contract No. MFPR 2005 on the mechanistic code MFPR development; the personal support and collaboration of Drs R. Dubourg and P. Giordano (IRSN) are highly appreciated.

This work was also supported by the Russian Foundation for Basic Research which is greatly acknowledged by the author.

References

[1] L. Bourgeois, Ph. Dehaudt, C. Lemaignan, J.P. Fredric, J. Nucl. Mater. 295 (2001) 73.
[2] J.R. McEwan, J. Am. Ceram. Soc. 4 (1962) 37.
[3] R.L. Goble, J. Appl. Phys. 32 (1961) 793.
[4] W.D. Kingery, B. Francois, J. Am. Ceram. Soc. 48 (1965) 546.
[5] F.A. Nichols, J. Am. Ceram. Soc. 51 (1968) 468.
[6] R.J. Brook, J. Am. Ceram. Soc. 52 (1969) 36.
[7] R.J. Brook, in: F.F. Waing (Ed.), Treatise Materials Science Technology, Ceramics, vol. 9, Academic Press, New York, 1979, p. 331.
[8] R.J. White, M.O. Tucker, J. Nucl. Mater. 118 (1983) 1.
[9] M.V. Speight, W. Beere, Met. Sci. 9 (1975) 190.
[10] G.B. Alcock, R.J. Hawkins, A.W.D. Hills, P. McNamara, Paper SM-66/36, IAEA, Symp. Thermodynamics, Vienna, 1965, p. 57.
[11] P.S. Maiya, J. Nucl. Mater. 40 (1971) 57.